Longitudinal Beam Dynamics of a Rapid Cycling Synchrotron Demonstrator

Oliver Smedt

August 2024

Supervised by Fabian Batsch and Leonard Thiele

Abstract

A Muon collider is an innovative idea for a lepton accelerator not constrained by synchrotron radiation. The fast decay of the muons necessitates quick acceleration, and hence fast ramp rates of the bending magnets. For this purpose a new synchrotron design has been proposed dubbed the hybrid rapid cycling synchrotron, which would combine super conducting and normal conducting magnets. This new design is quite different from a regular synchrotron as the path of the synchronous particle would vary during the acceleration. For this reason it has been suggested to build a demonstrator facility which would test the hybrid magnet layout. In the demonstrator the super conducting magnets would be replaced with normal conducting ones so that after its original purpose, the facility could be changed to a regular synchrotron and become a user facility or be used as an injector for a storage ring. In this report we simulate the longitudinal beam dynamics of the demonstrator and the effects of beam loading in its user mode using a set of assumed parameters. It is found that the Tesla cavities planned to be used in the actual muon collider would experience strong beam loading, and other cavities may be better suited. Additionally the bunch length may be limited due to the effect of quantum excitations.

Contents

1 Introduction

Multiple plans are currently under discussion for upcoming accelerators to supercede the LHC such as CLIC [1], FCC [2] and the International Muon Collider Collaboration (IMCC) [3]. Among these, the IMCC stands out as an interesting attempt to build a high energy lepton collider for muons. The use of muons makes this machine quite different from other lepton synchrotrons such as the LEP or FCC-ee, as the maximum energy would no longer be limited by synchrotron radiation. Instead, the extremely short half life of the muon would be a challenge. Bringing muons to the desired energy before they decay will require a series of rapid cycling synchrotrons (RCS) making use of fast acceleration and thus time dilation. The fast acceleration sets high criteria for the bending magnets that must both have high maximum field strength and fast ramp rates. For this reason a new magnet layout has been proposed, mixing fixed field super conducting magnets and fast ramping regular conducting magnets into one design (Hybrid RCS) [4]. To test the feasibility of such a magnet layout, a small scale demonstrator facility is proposed to be built, with the superconducting magnets represented by normal conducting magnets kept at fixed field for simplicity. This would be a small-scale electron accelerator which could be used for other research after its construction, i.e. be utilised as a user facility or as injector into an electron storage ring. In the user mode, all magnets would be ramped like in a regular synchrotron, and accelerate the electrons up to 3 GeV before passing them on to another machine or fixed target experiment. The aim of this project is to simulate the longitudinal dynamics of such an accelerator in its user mode using the in-house python-based macro-particle tracking code BLonD [5]. As no studies have been done on such a hybrid RCS demonstrator, we will assume a range of parameters and test the feasibility of these.

2 Longitudinal Dynamics Basics

In this section we look at a few key concepts in longitudinal beam dynamics, such as the phase space, momentum compaction factor, separatrix, and tracking, lending heavily from the JUAS lectures [6] and Accelerator physics by S. Y. Lee [7]. For further, detailed explanations, we invite the reader to read these references. The goal is to derive the kick and drift equations used in BLonD for particle tracking.

In its most basic form, a synchrotron concists of curved sections wherein the path of the particles is bend by dipole magnets, and RF cavities wherein the particles are accelerated by an oscillating electric field. Within the bending magnets, the radius of curvature ρ is governed by the magnetic rigidity formula

$$B_y\rho = \frac{p}{q} \Rightarrow p[\mathrm{GeV/c}] \approx 0.3ZB_y[\mathrm{T}]\rho[\mathrm{m}], \tag{1}$$

where B_y is the magnetic field, p is the momentum of the particle, q is the charge of the particle, $Z = q/e$ where e is the electron charge, and c is the speed of light in vacuum. In a synchrotron the bending radius is kept constant by keeping the magnetic field synchronous with the momentum. We dub the particle which has the right momentum to match our current magnetic field the synchronous particle.

Upon entering an RF cavity, a particle gains a different amount of energy based on its time of arrival as the field is oscillating. The field oscillates sinusoidally with an angular frequency ω_{RF} equal to a harmonic h times the angular revolution frequency $\omega_{rev,s}$ of the synchronous particle. This leads to an energy gain δE given by:

$$\delta E = qV_{RF}\sin\phi, \tag{2}$$

where V_{RF} is the amplitude of the oscillating cavity field and ϕ is the arrival phase of the particle. For this formula we assume that V_{RF} is correctly scaled to account for the variation in field strength as the particle passes the cavity. Note that $\omega_{rev,s}$ will vary as the synchronous particle is accelerated and ω_{RF} is tuned accordingly. This keeps the arrival phase of the synchronous particle ϕ_s constant. For ultra relativistic cases, this shift in RF frequency is relatively small, of the order kHz.

The difference in energy gain $\delta\Delta E$ between a given particle and a synchronous particle is:

$$\delta\Delta E = qV_{RF}\left(\sin\phi - \sin\phi_s\right). \tag{3}$$

A particle entering a curved section with a non-synchronous momentum will be travelling at a different speed and along a different trajectory than the synchronous particle. Hence its phase upon arrival at the next RF station will change. The change in trajectory can be described by the momentum compaction factor α. For a trajectory with circumference C we have:

$$\alpha \equiv \frac{dR/R}{dp/p}, \tag{4}$$

where $R = C/(2\pi)$ is the average radius of the trajectory. The momentum compaction factor is generally taken to be a constant of the accelerator[1]. To calculate the offset in phase, we can relate the momentum compaction factor to the phase slip factor η:

$$\eta \equiv -\frac{d\omega_{rev}/\omega_{rev}}{dp/p} = \frac{dR/R - d\beta/\beta}{dp/p} = \alpha - \frac{1}{\gamma^2}, \tag{5}$$

where β is the relativistic beta, γ is the relativistic gamma factor and ω_{rev} is the angular revolution frequency of the non synchronous particle. In the above equalities we have made use of the relations $\omega_{rev} = \beta c/R$ and $d\beta/\beta = 1/\gamma^2$. Interestingly η changes sign when $1/\gamma^2 = \alpha$. Above this γ, the change in path length will dominate over the change in speed. Thus a higher energy particle will arrive later at the next RF station. We denote this transition value as γ_t:

$$\gamma_t = \frac{1}{\sqrt{\alpha}}. \tag{6}$$

Using the phase slip factor, we can calculate a change in phase $\delta\phi$ over one turn, given some offset in energy from the synchronous particle ΔE. The derivative of the RF phase is given by:

$$\dot{\phi} = -h\left(\omega_{rev} - \omega_{rev,s}\right) = -h\Delta\omega, \tag{7}$$

where $\Delta\omega$ is the difference in angular revolution frequency between the synchronous and non synchronous particle. Multiplying by the revolution time $t_{rev,s}$ we can find the change in phase over one turn and derive an expression for $\delta\phi$ in terms of ΔE:

$$\Rightarrow \delta\phi = -h\Delta\omega t_{rev,s} = -2\pi h\Delta\omega/\omega_{rev,s} = 2\pi h\Delta\omega/\omega_{rev,s} = 2\pi h\eta\Delta p/p_s = \frac{2\pi h\eta\Delta E}{\beta^2 E_s}, \tag{8}$$

where p_s, E_s are synchronous momentum and energy respectively and Δp is the momentum offset from the synchronous particle. In the equalities above we have made use of the relation $\beta^2 dp/p = dE/E$. By combining equations 3 and 8 we have a set of equations of motion for non-synchronous particles in a synchrotron.

To track the particle with BLonD we first give it a 'kick' in the RF station using equation 3, then update its energy as $\Delta E_{new} = \Delta E_{old} + \delta\Delta E$. We then let it 'drift' in the bending field using equation 8, and similarly update the RF phase $\phi_{new} = \phi_{old} + \delta\phi$. Repeating this process over many turns, we can track the particle in the phase space spanned by ϕ and ΔE. For this project we will be working with the arrival time rather than RF phase $\Delta t = \phi/(\omega_{RF})$.

An example of particles moving in phase space can be seen on figure 1. Particle one is within a stable part of the phase space and orbits around the synchronous particle on a closed trajectory. Particle two is outside the stable phase space, and travels ahead of the synchronous particle. The stable and unstable regions of the phase space are separated by the so-called separatrix. A closed area within the separatrix is called an RF bucket. The separatrix itself is a function of the current synchronous energy and hence changes slowly during acceleration. It will also vary due to adverse effects such as induced voltages and synchrotron radiation.

A useful measure of beam quality is that of the emittance ϵ. The emittance of a particle is defined as the area enclosed by its trajectory. For a large bunch of particles we can estimate the emittance of the particles using:

$$\epsilon \approx 4\pi\sigma_{\Delta E}\sigma_{\Delta t}, \tag{9}$$

where $\sigma_{\Delta E}$, and $\sigma_{\Delta t}$ refer to standard deviation in energy offset and arrival time. The emittance should be preserved during acceleration and cannot easily be reduced except during special processes, see section 4.

[1] This is not always the case. For some accelerator optics the momentum compaction is a function of the particle momentum, and we have to do an expansion around the synchronous momentum $\alpha = \alpha_0 + \alpha_1 \frac{\Delta p}{p_s} + ...$ This complicates the dynamics slightly as each particle in the accelerator has different momentum compaction factor at every turn. But $\frac{\Delta p}{p_s}$ is generally small so we can truncate at zeroth order $\alpha \approx \alpha_0$.

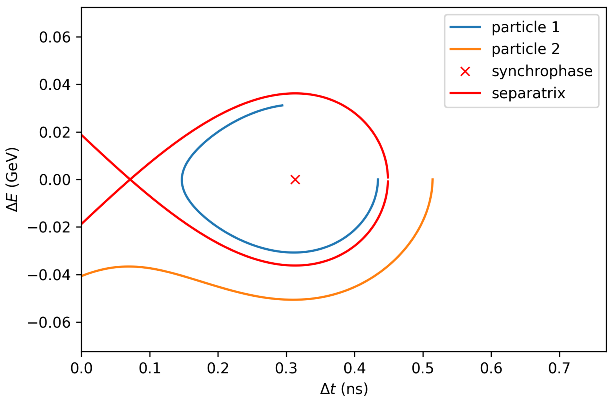

Figure 1: Example simulation for two electrons undergoing acceleration with $\phi_s = 3.79$ radians, $V_{RF} = 1\,\mathrm{MV}$, and initial energy of $1\,\mathrm{GeV}$ being accelerated for 217 turns. The RF frequency is $f_{RF} = 1.3\,\mathrm{GHz}$ and the harmonic is $h = 217$.

3 Specifications & Assumptions

In this section we will assume a variety of specifications for the RCS demonstrator as a starting point, and then throughout the report see whether the accelerator would work, or needs changed parameters.

The RCS demonstrator would be a smaller-scale synchrotron accelerating electrons from 0.1 GeV to 3 GeV. The saturation of the iron in the NC magnets sets a maximum bending field of 1.8 T. From limitations of the magnet powering the maximum ramp rate is 4 kT/s [8]. The magnet layout and optics will decide the momentum compaction factor, but no work has been done on the transverse dynamics. Determining the momentum compaction factor is therefore outside the scope of this project. As a reasonable placeholder value we will choose the value of the BESSY II electron storage ring at the Helmholtz-Zentrum Berlin of $\alpha = 7.3 \times 10^{-4}$ [9]. We make this choice as BESSY II is of similar size and energy. Not all of the length of the accelerator can be used for bending the beam. We denote the fraction used for bending the beam as the magnetic pack fraction and assume it to be 0.7. Given the injection energy, it is immediately possible to see that in this accelerator, we are always far above γ_t and in the highly relativistic regime.

$$\gamma_{inj} = \frac{E_{inj}}{m_e c^2} = 196 > \gamma_t = \frac{1}{\sqrt{\alpha}} = 37 \tag{10}$$

$$\gamma = 196 \to \beta = 0.99998 \approx 1 \tag{11}$$

The acceleration voltage is assumed to be provided by a single Tesla cavity [10], with an RF frequency of 1.3 GHz. This also sets the shunt resistance and quality factor used to model the fundamental mode of the cavity resonance model in section 5. For the beam input we can assume something similar to the beam provided by the CERN large electron accelerator for research (CLEAR) [11] or the beam stored in BESSY II [9]. This sets a bunch intensity of 1.2×10^{10} and an initial bunch length of order pico-seconds, for which we assume 5 ps. The assumed specifications of the accelerator are summarised in table 1.

From the maximum value of the magnetic field it is possible to immediately specify the minimum length of the accelerator. Using equation 1 and the fact that the bending radius is given by $R_{mag}C/(2\pi)$ we find that:

$$C = \frac{2\pi p[GeV/c]}{0.3 B_y[t] * R_{mag}}. \tag{12}$$

Assuming we reach the maximum allowed B field at the final turn with an energy of 3 GeV, we find that the allowed circumference is approximately 50 m. Since we are operating far above the rest mass energy of the electron, the speed can for the most part be assumed to be the speed of light. Thus the length of the accelerator alone decides the revolution time of the particle. The RF frequency should be an integer multiple of the revolution frequency, hence we should round up the circumference. That is to say, we want the lowest possible harmonic number such that $C = \frac{hc}{f_{RF}} > 50\,\mathrm{m}$. This is satisfied for $h = 217$ in which case $C = 50.042\,\mathrm{m}$. For the user mode we would like to accelerate multiple bunches, here we pick 7 bunches, as its a divisor of h. This gives a total beam current of 80 mA.

With the size defined we can use the maximum B-field ramp rate to determine the minimum number of turns required. Taking the derivative of equation 1, with constant bending radius and using the fact that $\beta \approx 1$, we find that the energy gain per turn and the derivative of the magnetic field are related by

Table 1: Pre-decided specification of RCS-demonstrator

Injection energy (E_{inj})	0.1 GeV
Extraction energy (E_{ext})	3 GeV
Momentum compaction factor (α)	7.3×10^{-4}
Magnetic pack fraction (R_{mag})	0.7
Maximum bending field (B_{max})	1.8 T
Maximum magnetic ramp rate ($\dot{B}_{max}$)	4 kT/s
RF-frequency (f_{RF})	1.3 GHz
RF-voltage (V_{RF})	30 MV
Cavity loaded quality factor (Q_L)	3×10^6
Cavity shunt impedance (R/Q)	518 Ω
Injected bunch length ($4\sigma_{\Delta t}$)	5 ps
Intensity per bunch	1.2×10^{10}

$$\delta E[GeV] = 0.3Z\frac{dB_y}{dt}[T/s]\frac{C^2[m^2]R_{mag}}{2\pi}. \tag{13}$$

Substituting in the maximum derivative of the magnetic field we find that $\delta E = 1.11\,\mathrm{MeV}$, and hence to complete the acceleration we need at least $(E_{ext} - E_{inj})/\delta E = 2600$ turns. The parameters determined by minimising the size and acceleration time can be seen in table 2.

Table 2: Additional specifications of RCS-demonstrator of minimal size and acceleration time

Circumference (C)	50.042 m
Harmonic number (h)	217
Energy gain per turn (δE)	1.11 MeV
Number of turns	2600
Beam current (i_b)	80 mA
Number of bunches	7
Synchrophase (ϕ_s)	3.10 rad

At this point it is possible to simulate the longitudinal dynamics of the accelerator. However, to make the simulation realistic we must consider adverse effects such as impedance and synchrotron radiation as well.

4 Synchrotron Radiation & Quantum Excitation

An accelerated charge will radiate energy perpendicular to its direction of acceleration. In a synchrotron where particles are forced on a circular path and therefor accelerated towards the centre of curvature, this leads to radiation along the direction of travel, which will reduce the energy of the particles. The emitted power per meter for an electron beam is given by [12]:

$$\frac{dP}{ds}[\mathrm{W/m}] = 14.1\frac{E^4[\mathrm{GeV}^4]i_b[\mathrm{mA}]}{\rho^2[\mathrm{m}^2]}, \tag{14}$$

where i_b is the current of the beam. By assuming constant power loss during a turn and particles travelling at close to the speed of light, we can derive that the energy loss per particle per turn is given by:

$$\delta E_{synch}[\mathrm{MeV}] = 0.557\frac{E^4[\mathrm{GeV}^4]}{R_{mag}C[\mathrm{m}]}. \tag{15}$$

At flat top this leads to a loss in energy of around 1.3 MeV per turn. This is comparable to the necessary energy gain per turn for fast acceleration and a not insignificant fraction of the maximum 30 MeV the Tesla cavity can provide per turn. This effect is not negligible and must be accounted for in simulation. Synchrotron radiation consists of photons with quantized energy. The energy carried off by these photons can vary stochastically. This leads to an effect known as quantum excitation, in which the bunch will gain emittance due to the random energy loss of its constituent particles. For a beam stored at constant energy, the effect of synchrotron radiation can be seen on figure 2.

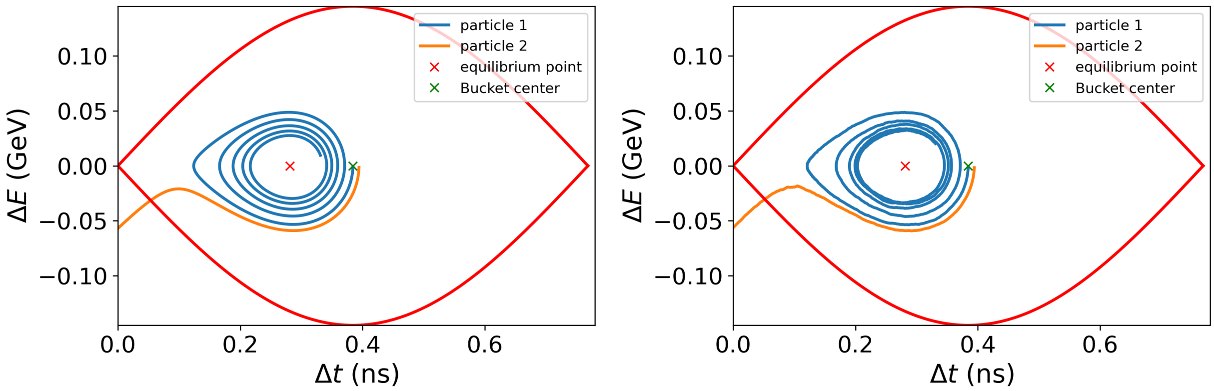

Figure 2: Path of two particles with no acceleration, but subject to synchrotron radiation with (right) and without (left) quantum excitation. The particles are electrons kept at 3 GeV in a 50m accelerator with an RF voltage of 1.74 MV, a magnetic pack factor of 0.7, a harmonic number of 217, and $\alpha = 7.3 \times 10^{-4}$. The separatrix, shown as a red line, does not consider the effect of synchrotron radiation.

The new synchronous phase is at the point where the energy gained by the RF exactly matches the energy loss due to synchrotron radiation, referred to as 'equilibrium point' in figure 2. Due to the increased energy loss of particles with a surplus of energy as opposed to those with a lack of energy, there is a cooling effect that allows the emittance to shrink, known as radiation damping [7]. Without the effect of quantum excitation, the emittance would shrink until all particles are in the same place in phase space. With quantum excitations the emittance will reach an equilibrium point. It is also important to note the shrinking of the real separatrix. If the RF voltage exactly matched the loss from synchrotron radiation, there would only be a single stable point in phase space. Hence synchrotron radiation reduces the size of the bucket.

5 Cavity Impedance

Upon passing the RF cavity, the bunch will induce an electric field known as a wake field. This will absorb some energy from the bunch and induce a time dependent voltage on any bunch arriving at a later time. Studying the impedance model behind these wake fields for existing accelerators is an important topic, see for instance [13]. However, it requires either knowledge of the geometry of the accelerator components or real world measurements to obtain the impedance spectra. For the purposes of the RCS demonstrator, the only impedance source we already have knowledge off is that of the RF cavity. We can model it as a series of RLC circuits attached to a current source. The impedance model is then characterised by the loaded quality factor, resonant frequency, and shunt resistance of these RLC circuits. One of these RLC circuits corresponds to the fundamental mode of the cavity at or around ω_{RF}. The other modes at higher frequency are referred to as higher order modes (HOM). Parameters of two HOMs of the Tesla cavity can be seen on table 4.

Table 3: Parameters used for the two most prominent HOMs of the Tesla cavity [8].

Parameter	HOM 1	HOM 2
Shunt impedance (R/Q)	$7.44\,\Omega$	$77.6533\,\Omega$
Loaded quality factor (Q_L)	5.35×10^5	4.75×10^5
Resonance frequency (f_r)	$2.4419\,\mathrm{GHz}$	$2.4499\,\mathrm{GHz}$

Since the the loaded quality factors for the Tesla cavity are significantly larger than the harmonic number of the RF ($Q_L >> h$), it is apparent that the wake of any bunch will last long enough to interfere with the same bunch on subsequent turns. Hence multi turn effects must be considered.

In BLonD this is a challenge for our use case. In BLonD's standard wake field implementation the induced voltage is tracked as a time series, at the same resolution as the bunch profile. Since the bunch length is of order pico seconds, and the wake lasts for around $Q_L/(\pi f_{RF}) \approx 0.7\,ms$ [14], we can see it would require around $10^{-3}s/10^{-12}s = 10^9$ data points in the time series of the induced voltage. This array would thus require a few Gigabytes of RAM, which can't easily be computed and stored on the available computing resources. Instead we can assume a Gaussian bunch shape, and use the analytical expression of a Gaussian bunch passing a resonator, to calculate the induced voltage. This function is already implemented in BLonD [5]. With this approach we then evaluate the analytical function during bunch passage, skipping the need to calculate and store the entire time series of the induced voltage.

This does come with an inherent inaccuracy as the bunch is typically parabolic in shape and not Gaussian. But since the bunch length is very small compared to the period of the fundamental mode, it should appear to the impedance source as a point-like distribution in either case. Although this method reduces the memory overhead, it still needs to evaluate a couple of thousand induced voltage functions at many points in time, hence evaluation of these wakes makes a simulation of 2600 turns take around 8 hours when considering the fundamental mode plus two HOMs.

A particularly problematic resonance of the cavity is the fundamental mode at or around the RF frequency. Unless the cavity is de-tuned, the period of this mode will line up with the period between arriving bunches. This will ensure the phases of all the induced voltages are the same, allowing them to constructively build up over time. Since the fundamental mode will always have a high quality factor this build-up eventually becomes large enough to overpower the RF system and prohibit acceleration of the bunch. This effect is commonly referred to as beam loading [7] and a phasor diagram to show its effect with and without de-tuning can be seen on figure 3.

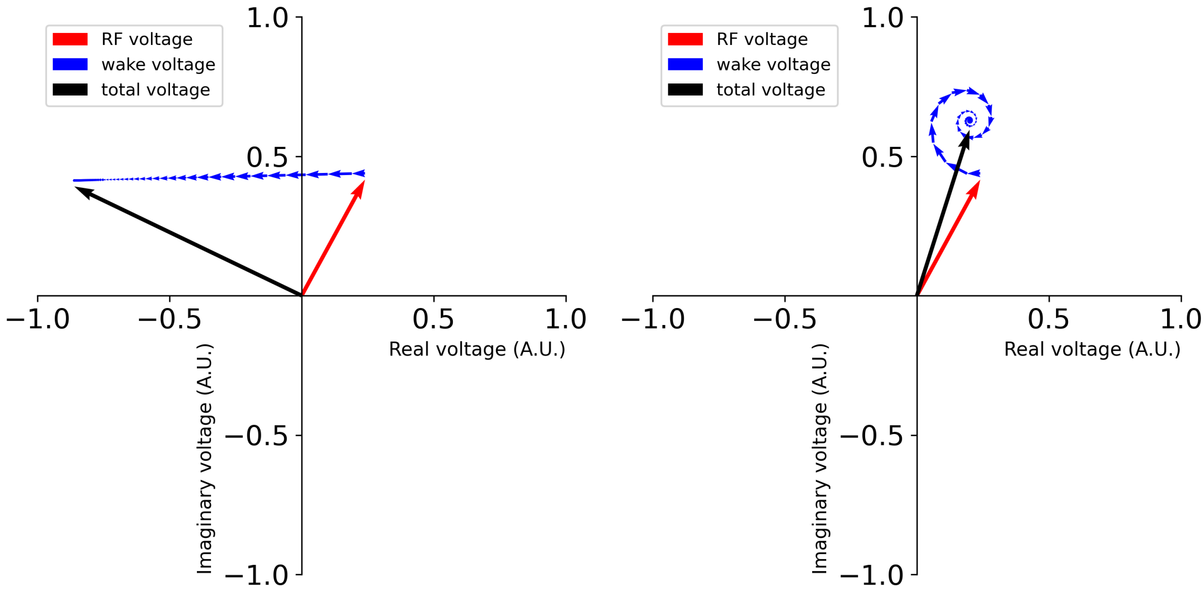

Figure 3: Illustrative example of how negatively de-tuning the cavity affects the voltage induced by the beam under the assumption of a steady state beam. Left shows the case without de-tuning. The induced voltages from previous bunch passes will build-up constructively until capped by their decay rate, in this case resulting in a decelerating voltage applied to the bunches. Right shows the case with de-tuning, here each wake phasor is slightly phase shifted, resulting in a total voltage closer to the RF voltage.

By carefully choosing the phase and amplitude of the driving current and picking the right de-tuning, it is possible to compensate for beam loading. For the steady state case of a continuous non changing beam of average current $I_{b,DC}$, the ideal de-tuning is given by [14]:

$$\frac{\Delta\omega_{opt}}{\omega_{RF}} = \frac{I_{b,DC}\cos(\phi_s)R/Q}{V}, \tag{16}$$

where $\Delta\omega_{opt}$ is the optimal de-tuning, and V is the voltage in the cavity. For our purposes we are not in the continuous case as we will start with zero induced voltage and have it gradually build up over time. Hence a fixed de-tuning will not keep the total voltage constant. For existing accelerators such as the LHC, complex feedback systems are in place to keep the voltage in the cavity constant. These feedback systems are outside the scope of this project, and so we will simple use equation 16 to find an ideal de-tuning and then keep the RF voltage from the generator fixed at what would be the ideal neglecting wakes. Using equation 16 the ideal de-tuning comes out to $\Delta\omega_{opt} = -1.7\,\mathrm{kHz}$. In addition to the so far described machine parameters, we can also reduce the total intensity per bunch for a beam current of 20 mA, which is the value planned for the actual Muon collider [8]. In this case the ideal de-tuning is $\Delta\omega_{opt} = -425\,\mathrm{Hz}$.

6 Simulation Results

6.1 Simulation with Tesla cavity

With everything combined it is possible to do a simulation that takes into account synchrotron radiation and three of the resonant modes of the cavity. This is done at 80 mA with no de-tuning and 20 and 80 mA with appropriate de-tuning. The simulation for 80 mA with no de-tuning after 1000 turns can be seen on figure 4.

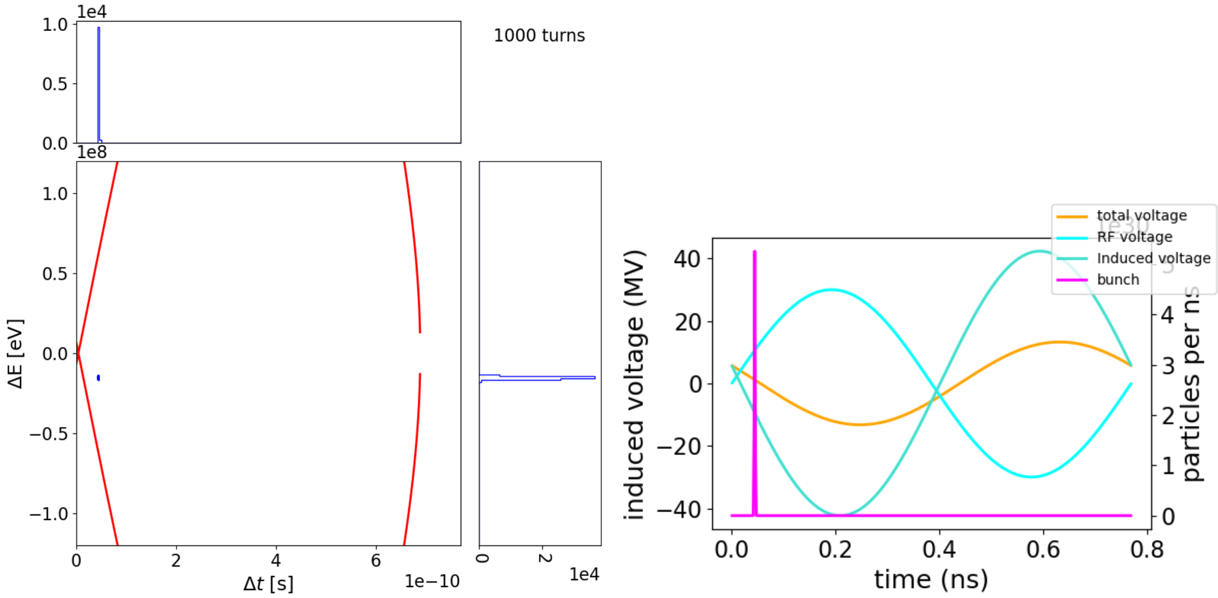

Figure 4: (left) Longitudinal phase space of the first bunch at turn 1000 for a tesla cavity with beam current of 80 mA and no de-tuning. (right) The induced voltages in the Tesla cavity at turn 1000. The shown separatrix is based on the RF voltage and does not consider the induced voltages.

It is clear that the total cavity voltage is phase shifted over time. This happens slowly enough that the bunch is able to move along with the total voltage. This phase shift is not necessarily an issue as the process to which the bunch is delivered at flat top can simply be matched in phase. However, the reduction in total cavity voltage might be an issue as the bunch will be lost if the cavity cannot provide the 1.11 MeV required per turn for the acceleration plus the 1.13 MeV emitted through synchrotron radiation per turn. De-tuning the cavity helps reduce this loss of voltage. This can be seen on figure 5.

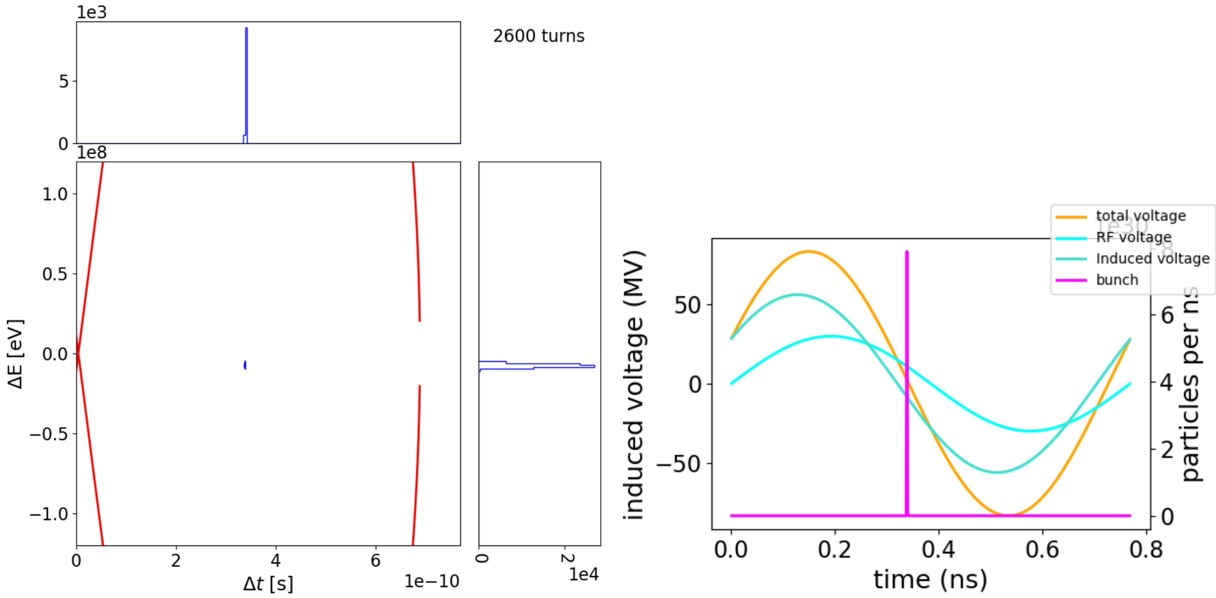

Figure 5: Simulation results for Tesla cavity with 80 mA beam current and optimal de-tuning of -1.7 kHz. (left) longitudinal phase space of the first bunch at flat top. (right) The induced voltages in the Tesla cavity at flat top. The shown separatrix is based on the RF voltage and does not consider the induced voltages.

The amplitude of the total voltage has increased above what is provided by the RF. This is due to the de-tuning and mirrors what is shown in figure 3. The phase is still shifted slightly, but significantly less than without de-tuning. By the end of the acceleration, the induced voltages had not yet reached a steady state.

In addition to the phase shift, there is also an emittance blow-up during the acceleration. This can be seen on figure 6. This growth is caused by intensity effects and should ideally be minimized.

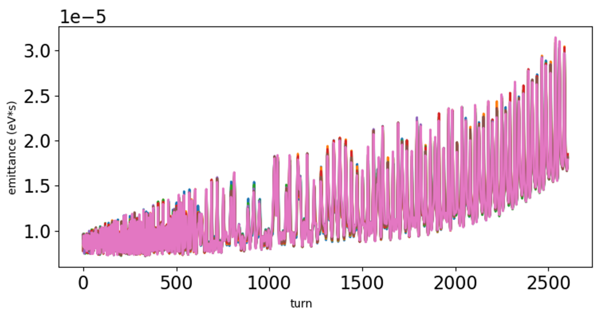

Figure 6: Emittance of the bunches during the acceleration for 80 mA. Emittance was calculated using equation 9.

We can redo these simulations again for a beam current of 20 mA expected in the Muon collider. The phase space at the end of the simulation can be seen in figure 7.

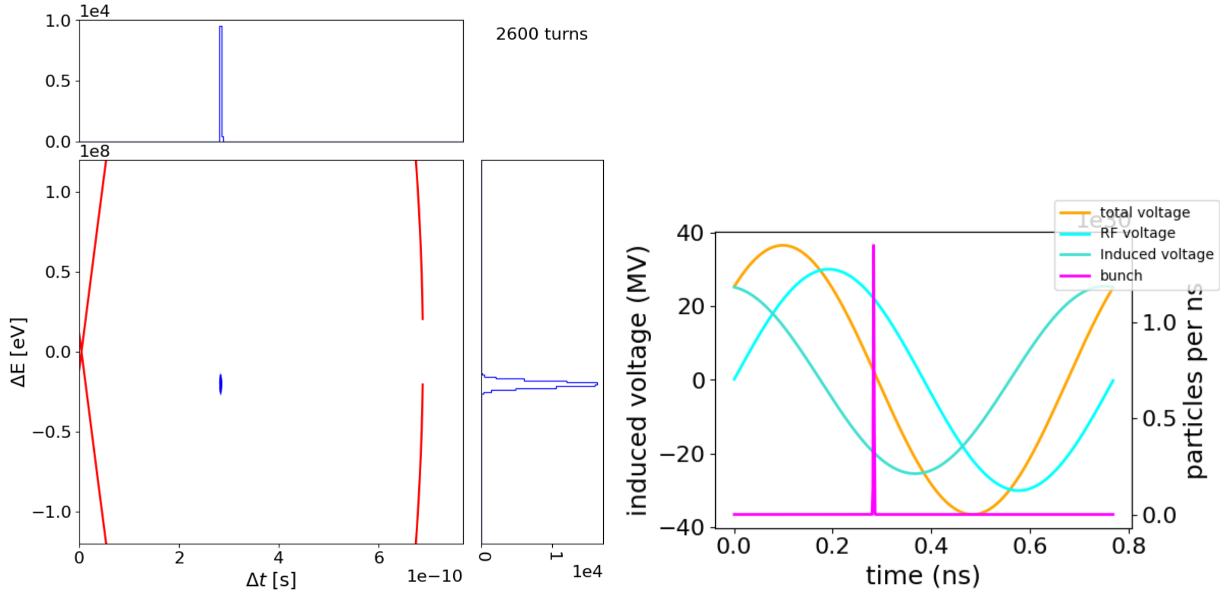

Figure 7: (left) Longitudinal phase space of the first bunch at flat top with 20 mA beam current and an optimal de-tuning of -425 Hz. (right) The induced voltages in the cavity at flat top. The shown separatrix is based on the RF voltage and does not consider the induced voltages.

The phase shift is greater as compared to 80 mA with 1.7 kHz de-tuning and the total cavity voltage is smaller due to weaker induced voltages. Like in the 80 mA case, there is an emittance blowup, see figure 8. It is caused by a mixture of quantum excitation and impedance effects. This blowup can be seen to vanish when starting with a longer bunch, in which case radiation damping is observed.

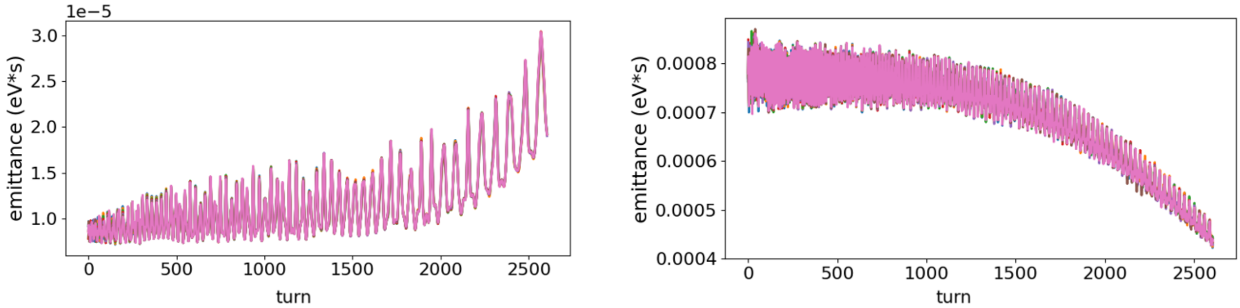

Figure 8: (left) Emittance of bunches during acceleration for 20 mA with de-tuning and 5 ps bunches. (right) Emittance during same acceleration for 50 ps bunches.

6.2 Repeating study for LEP2 cavities

As a very brief test of another cavity we can see if a module of LEP2 cavities would be able to better handle the planned intensity per bunch of 1.2×10^{10}. The change of cavities necessitates a slight change of accelerator parameters. The change in RF frequency changes the accelerator length to 51.07 m for a harmonic number of 60. Seven is no longer a divisor of the harmonic so we will switch to 6 bunches, giving a current of 69 mA. The total time spent to accelerate the bunches is kept the same, resulting in slightly fewer turns due to the longer circumference. The changed parameters are shown in table 4.

Table 4: Updated parameters for simulation with LEP2 cavities. The basic specs of the cavities themselves can be found in [15]. No HOM were considered for these cavities.

RF voltage (V_{RF})	$10.2\,\mathrm{MV}$
RF frequency (f_{RF})	$352\,\mathrm{MHz}$
Loaded quality factor (Q_L)	2.2×10^6
Shunt impedance (R/Q)	$232\,\Omega$
Circumference (C)	$51.07\,\mathrm{m}$
Harmonic number (h)	60
Energy gain per turn (δE)	$1.13\,\mathrm{MeV}$
Number of turns	2553
Beam current (i_b)	$69\,\mathrm{mA}$
Number of bunches	6
De-tuning ($\Delta\omega_{opt}$)	$-544\,\mathrm{Hz}$

The longitudinal phase space on the final turn and the cavity voltages can be seen on figure 9. The phase shift is comparable to the simulation with the Tesla cavity and the induced voltages have a similar constructive effect with the higher intensity.

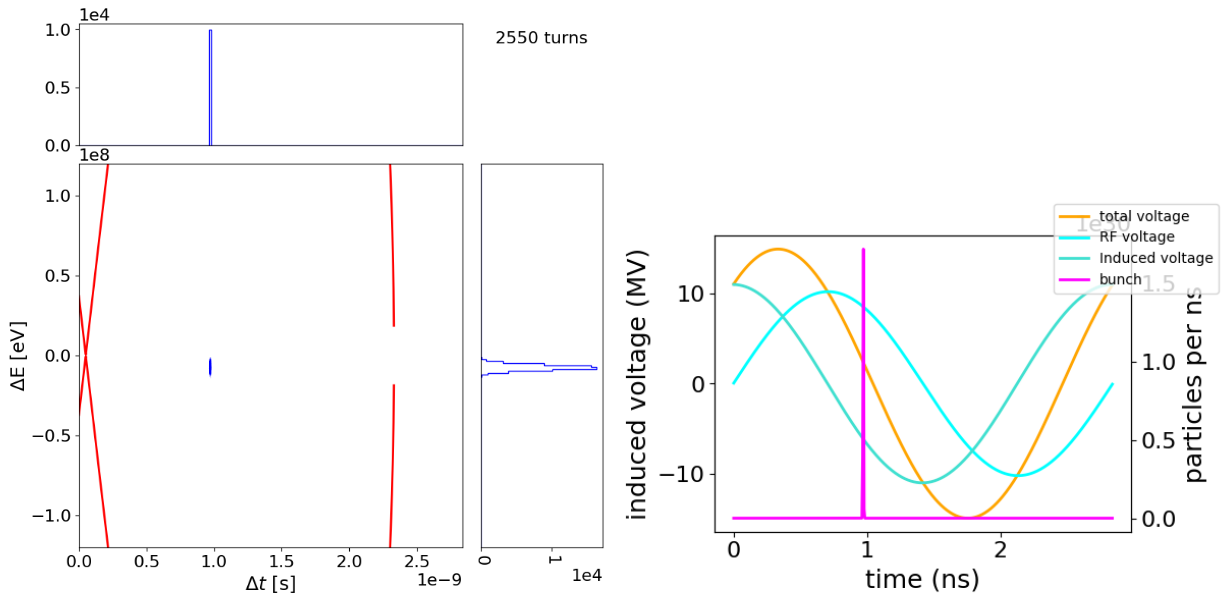

Figure 9: (left) longitudinal phase space of the first bunch at the end of the acceleration for the LEP cavity simulation. (right) The induced voltages in the LEP cavity at the end of the acceleration. The shown separatrix is based on the RF voltage and does not consider the induced voltages.

The emittance of the bunch during acceleration can be seen on figure 10. The LEP cavity seems to experience a similar emittance blowup as the Tesla cavity. Removing the effect of quantum excitations reveals that the blowup later in the acceleration is due to being below the equilibrium emittance of the synchrotron radiation. With this removed we can still see an increase in emittance caused by intensity effects.

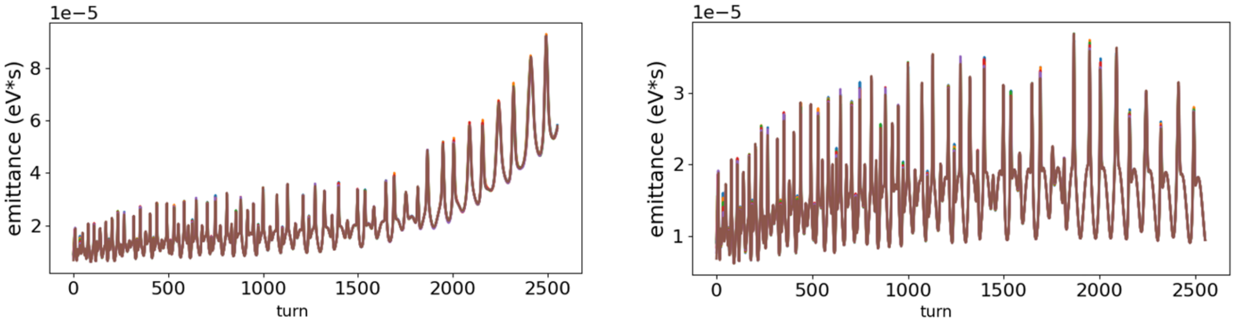

Figure 10: (left) Emittance of the bunchs during the acceleration. (right) Emittance during acceleration but with quantum excitations turned off.

7 Discussion & Conclusion

Simulations of the RCS demonstrator in user mode given the specifications in section 3, show that the accelerator would be heavily affected by beam loading. For the Tesla cavity a bunch of length 5 ps experienced significant emittance growth due to both intensity effects and quantum excitation. A 50 ps bunch was stable for a 20 mA beam, indicating that a sweep for ideal bunch lengths at different beam currents would be beneficial. The results for the LEP cavity were similar, with a 5 ps bunch also growing in emittance for this cavity.

The growth due to quantum excitation is unavoidable without faster acceleration. The acceleration rate is however limited by the ramping rate of the fast-ramping magnets. The growth due to intensity effects might be avoidable. It should be noted that 80 mA is low compared to the beam current of the BESSY II of 300 mA [9], which has order ps bunch lengths as well. Hence better choice of cavities and considerations of feedback systems would likely improve the possible bunch length. For further research in this direction it would be beneficial to study normal conducting cavities as the 30 MV provided by the Tesla cavity is not necessary for this machine.

These simulations did not make any assumptions with regards to the injection and extractions schedules of the accelerator. These would be important due to the intensity effects as the injection would dictate the induced voltages at the start of the acceleration and the voltages would keep building up at flat top. Hence assumptions regarding these schedules would be beneficial in the future.

Lastly for a more accurate simulation, the optics and magnet layout would need to be determined to specify the correct momentum compaction factor. This would also be of interest if we want to simulate the accelerator while using its hybrid magnet scheme, since the magnet layout in hybrid RCS mode would induce a change in path length as a function of synchronous energy.

8 Acknowledgements

At CERN I stand on the shoulders of giants without whom this project would not have been feasible. In particular, I would like to thank Alexandre Lasheen for his notes on longitudinal beam dynamics and suggestion to compute the induced voltage analytically. I would also like to thank Ivan Karpov, Birk Karlsen-Baeck and Heiko Damerau for their input on beam loading and how to mitigate it. Lastly this project would not have been possible without Fabian Batsch and Leonard Thiele who provided some of the basic specifications of the RCS demonstrator and decided the direction of the project.

References

[1] M. Aicheler et al. *The Compact Linear Collider (CLIC) – Project Implementation Plan*. Ed. by M. Aicheler. CERN Yellow Reports: Monographs. 247 p. 2018. DOI: 10.23731/CYRM-2018-004. URL: https://cds.cern.ch/record/2652600.

[2] A. Abada et al. “FCC-ee: The Lepton Collider”. In: *The European Physical Journal Special Topics* 228.2 (June 2019), pp. 261–623. ISSN: 1951-6401. DOI: 10.1140/epjst/e2019-900045-4. URL: https://doi.org/10.1140/epjst/e2019-900045-4.

[3] C. Accettura et al. *Interim report for the International Muon Collider Collaboration (IMCC)*. Tech. rep. This document summarises the International Muon Collider Collaboration (IMCC) progress and status of the Muon Collider RD programme. 2024. arXiv: 2407.12450. URL: https://cds.cern.ch/record/2904891.

[4] F. Batsch et al. "Longitudinal beam dynamics and RF requirements for a chain of muon RCSs". In: *Proc. IPAC'23* (Venice, Italy). IPAC'23 - 14th International Particle Accelerator Conference 14. JACoW Publishing, Geneva, Switzerland, May 2023, pp. 1428–1431. ISBN: 978-3-95450-231-8. DOI: 10.18429/JACoW-IPAC2023-TUPA040. URL: https://indico.jacow.org/event/41/contributions/1602.

[5] H. Timko et al. "Beam longitudinal dynamics simulation studies". In: *Phys. Rev. Accel. Beams* 26 (11 Nov. 2023), p. 114602. DOI: 10.1103/PhysRevAccelBeams.26.114602. URL: https://link.aps.org/doi/10.1103/PhysRevAccelBeams.26.114602.

[6] A. Lasheen. "Longitudinal beam dynamics". In: Proceed- ings of the Joint Universities Accelerator School (JUAS): Courses and exercises, E. Métral (ed.) CERN Yellow Reports: School Proceeding, to be published.

[7] S. Y. Lee. *Accelerator Physics*. 3rd ed. World Scientific Publishing, 2012.

[8] F. Batsch and L. Thiele. *internal communications*. 2024.

[9] A. Jankowiak et al. "The Bessy VSR Project for short X-ray pulse production". In: *Proc. IPAC'16* (2016), pp. 2833–2836.

[10] B. Aune et al. "Superconducting TESLA cavities". In: *Phys. Rev. ST Accel. Beams* 3 (9 Sept. 2000), p. 092001. DOI: 10.1103/PhysRevSTAB.3.092001. URL: https://link.aps.org/doi/10.1103/PhysRevSTAB.3.092001.

[11] K. N. Sjobak et al. "Status of the CLEAR electron beam user facility at CERN". In: *Proc. IPAC'19* (2019), pp. 983–986.

[12] R. Bailey et al. "Synchrotron Radiation Effects at LEP". In: (1998). URL: https://cds.cern.ch/record/360833.

[13] M. Zampetakis et al. "Refining the LHC Longitudinal Impedance Model". In: *JACoW HB* 2023 (2024), pp. 559–562. DOI: 10.18429/JACoW-HB2023-THBP37. URL: https://cds.cern.ch/record/2900891.

[14] J. Tückmantel. "Cavity-Beam-Transmitter Interaction Formula Collection with Derivation". In: (2010). URL: https://cds.cern.ch/record/1323893.

[15] *LEP design report*. Report. Geneva: CERN, 1984. URL: https://cds.cern.ch/record/102083.